Carbon Ion Radiation Therapy for Liver Tumors

14

Zheng Wang, Wei-Wei Wang, Kambiz Shahnazi, and Guo-Liang Jiang

Contents

Carbon ion radiation therapy (CIRT) facilities are available in Japan, Germany, and China. The National Institute of Radiological Science (NIRS) and Hyogo Ion Beam Medical Center (HIBMC), both institutions in Japan, have used CIRT to treat hepatocellular carcinoma (HCC) patients, and Heidelberg Ion Beam Therapy Center (HIT) in Germany has treated a limited number of patients. The outcomes of CIRT for HCC have been very encouraging. Shanghai Proton and Heavy Ion Center (SPHIC) has been using CIRT for HCC since 2014. In this section, we will address CIRT for HCC.

Z. Wang • W.-W. Wang • K. Shahnazi
G.-L. Jiang (✉)
Department of Radiation Oncology, Shanghai Proton and Heavy Ion Center, 4365 Kang Xin Road, Shanghai 201321, China
e-mail: guoliang.jiang@sphic.org.cn

N. Lee et al. (eds.), *Target Volume Delineation and Treatment Planning for Particle Therapy*, Practical Guides in Radiation Oncology,
https://doi.org/10.1007/978-3-319-42478-1_14

14.1 Physical Dose Distribution Comparison Between Proton and Carbon Ion

Similar to protons, the carbon ion beam possesses the same characteristics of physical dose distribution, such as the "Bragg peak"; however, compared to protons, the carbon ion "Bragg peak" is much steeper and the width narrower. In scan beam facilities, a ripple filter has to be used to widen the "Bragg peak" in order to decrease the number of scanned layers. In addition, the dose behind the "Bragg peak," called fragment tail dose, is slightly higher than that of proton dose tail. In other words, the carbon ion dose behind the "Bragg peak" is slightly larger than for protons (Fig. 14.1). Furthermore, the lateral penumbra of the carbon ion beam is smaller than that of the proton beam (Fig. 14.2). As a result, the carbon ion beam can deliver less dose to organs at risk (OARs), which are located laterally at the axis of the beam direction, but slightly more dose to OARs behind the target.

14.1.1 Hepatic Radiation Injury and Proliferation

For HCC irradiation, it is the consensus that the dose to uninvolved healthy liver is critical for the success of the radiotherapy. The most severe radiation complication is radiation-induced liver disease (RILD). Once RILD occurs, over 70% of patients will die of this fatal complication. Therefore the priority in HCC irradiation is to prevent RILD in these patients. Unfortunately, the majority of HCC patients are associated with hepatic cirrhosis, which is induced by hepatitis B virus in Asia, or in the western countries by hepatitis C, or alcohol abuse. Therefore, keeping the radiation dose as low as possible to the normal liver is the first priority when an HCC radiation plan is designed.

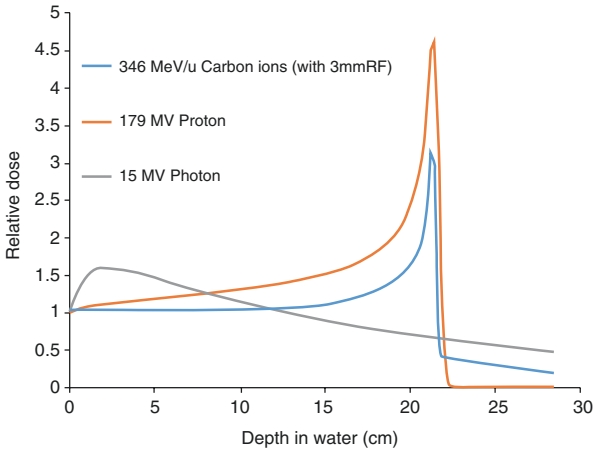

Fig. 14.1 Percentage depth dose distributions in water for 15 MV photon, 179 MeV proton, and 346 MeV/u carbon ion (with 3 mm ripple filter)

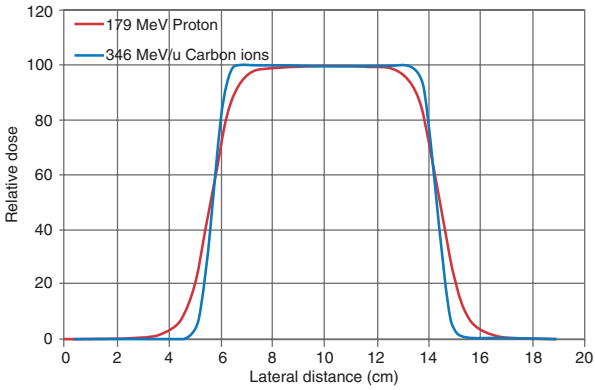

Fig. 14.2 The lateral penumbras of proton and carbon ion beams at the "Bragg peak" dose area

From previous photon experience reported in the literature for HCC irradiation, the mean dose to normal liver, defined as the whole liver volume minus GTV, is one of the most important parameters [1, 2]. After radiation-induced liver injury, the remaining healthy liver can be stimulated to repopulate significantly and could compensate for the lost hepatic function, which means the capability to proliferate in remaining healthy liver is also important in HCC irradiation. From animal studies on the liver, it was found that proliferation occurs after irradiation injury [3, 4, 5]:

(1) Unirradiated liver possessed a very strong capability to proliferate after hepatic radiation injury.
(2) The liver with low-dose irradiation also had the capability to proliferate, but the liver receiving higher dose had poorer capability to proliferate.
(3) The cirrhotic liver induced by chemicals could also repopulate, but its capability would be poorer than the normal liver [6].

However, in the clinic, it is very difficult to predict the hepatic capability of proliferation after different irradiation doses to different scales of cirrhosis at the current time. Therefore, a strategy should be to keep a part of the healthy liver totally unirradiated, the unirradiated healthy liver volume as much as possible, and the dose to healthy liver as low as possible. From the above considerations, protons and CIRT are superior to IMRT.

14.1.2 Clinical Relevance

Dose comparisons has been evaluated for three plans of therapy, photon intensity-modulated radiation therapy (IMRT), intensity-modulated proton therapy (IMPT), or intensity-modulated carbon ion therapy (IMCT), for each of eight HCC patients,

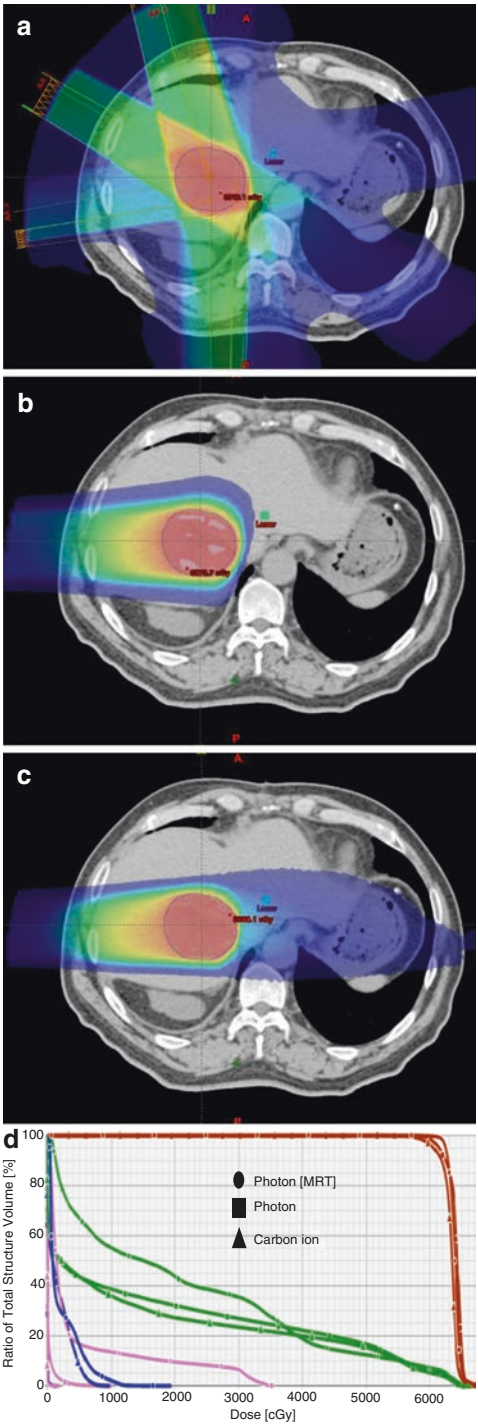

Fig. 14.3 Dose distribution comparison in a typical hepatocellular carcinoma patient. (**a**) Photon IMRT, (**b**) proton, and (**c**) carbon ion; (**d**) dose volume histogram for the target (ITV) (*brown line*), liver (*green line*), right kidney (*pink line*), and stomach (*blue line*). The ITV coverage, liver mean dose, kidney mean dose, and stomach maximum dose were 93.6%, 16.71 GyE, 0.20 GyE, and 1.60 GyE for proton; 90.3%, 15.23 GyE, 0.01 GyE, and 9.75 GyE for carbon ion; and 98.7%, 21.35 Gy, 4.84 Gy, and 19.57 Gy for photon IMRT, respectively

Table 14.1 Comparison of doses to the liver, right kidney, and stomach using IMRT, proton, and carbon ion beam from eight hepatocellular carcinomas

Dose parameter	Photon	Proton	Carbon
ITV coverage (V95%)	99.8 ± 3.2	99.6 ± 4.8	99.9 ± 3.7
Liver			
Mean dose (GyE)	23.17 ± 4.30*	17.00 ± 2.92$^{\#}$	15.49 ± 2.62$^{\$}$
Kidney			
Mean dose (GyE)	5.91 ± 10.7^{+}	2.84 ± 8.46$^{\&}$	2.00 ± 9.41$^{=}$
Stomach			
Max dose (GyE)	29.92 ± 7.10**	2.61 ± 13.55$^{\#\#}$	10.03 ± 12.79$^{\$\$}$

t test: * vs. #, $p = 0.00$; * vs. $, $p = 0.00$; # vs. $, $p = 0.01$; + vs. &, $p = 0.02$; + vs. =, $p = 0.01$; ## vs. $$, $p = 0.01$
For all other comparisons between two parameters, p were >0.05

who were finally irradiated with CIRT in our center. Figure 14.3 shows the dose distributions from one of the eight HCC patients irradiated by IMRT, proton beam, and carbon ion beam. Table 14.1 summarizes the doses to the tumor, liver, right kidney, and stomach from 8 HCC patients. To produce the same target coverage (95% of ITV covered by 95% of prescribed dose), proton and carbon ion beams deliver lower doses to the kidney and liver compared to IMRT for the same patient. Moreover, carbon ion beam delivers lower doses to the kidney and liver compared to protons because of smaller penumbra. However, due to the tail dose behind "Bragg peak," the stomach located distal to the target receives slightly higher dose with carbon ions compared to protons. Overall, CIRT has been shown to be more advantageous compared to protons with lower mean dose to the normal liver, which is the most important issue to reduce the hepatic toxicity, although the dose to stomach is slightly higher, which is likely negligible and will not produce stomach toxicity.

Because of the sharper penumbra of the carbon ion beam (Fig. 14.2), CIRT is more suitable for HCC patients if the tumor is located close to the gastrointestinal (GI) tract. Figure 14.4 demonstrates the dose distributions of proton and carbon ion treatment plans in one HCC patient. The lesion was close to duodenum, and the colon was embedded in the concave target. The dose volume histogram (DVH) in Fig. 14.4c shows that the doses delivered to the duodenum and colon by CIRT were lower than that by protons.

14.2 Radiobiological Effect Comparison Between Protons and Carbon Ions [7, 8, 9]

The biological effect of protons is a little higher than ^{60}Cobalt with relative radiobiological effect (RBE) of 1.0–1.1, but the carbon ion is different from proton. The RBE depends on beam LET. The LET of carbon ion is mixed with low LET in the entrance plateau dose and high LET in the area of the "Bragg peak." From preclinical experiments, it has been shown that 70% of DNA damage is the result of DNA

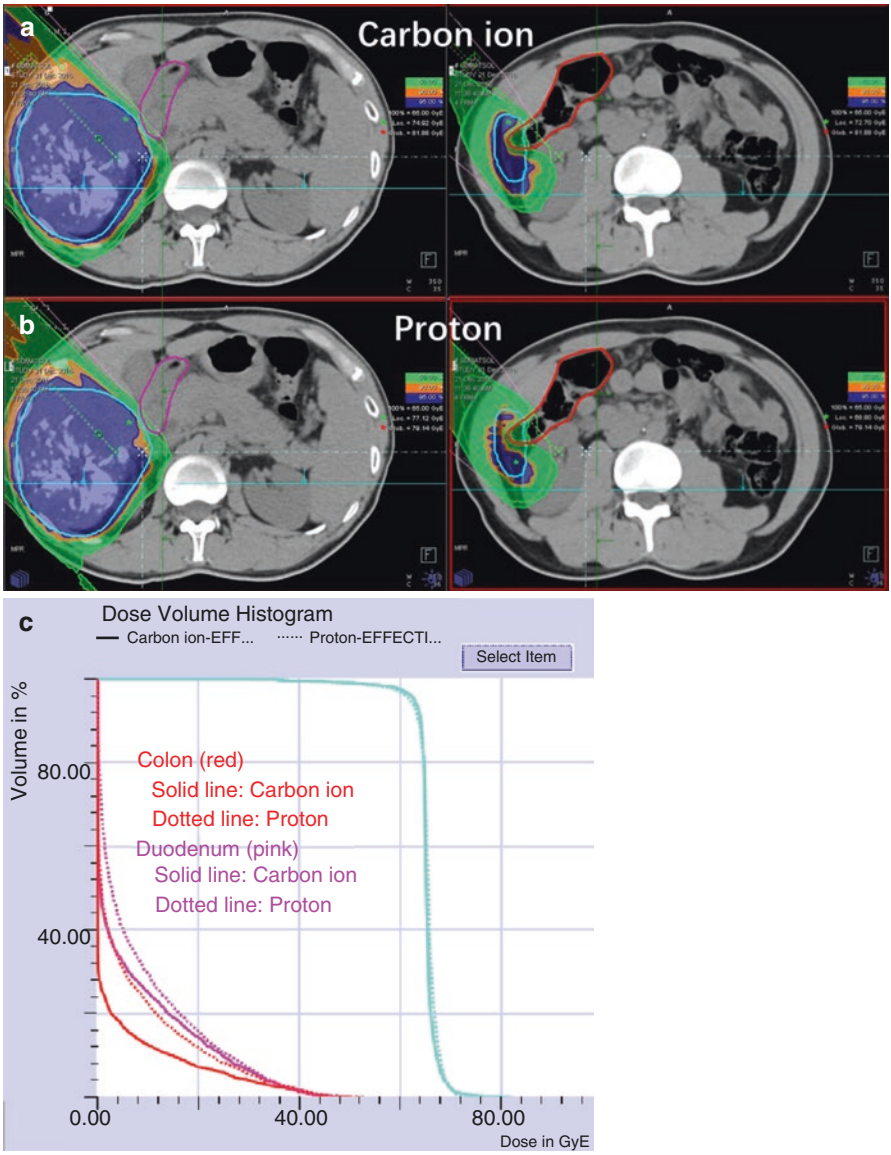

Fig. 14.4 Dose distribution for a hepatocellular carcinoma located close to the duodenum (*pink line*) and colon (*red line*), irradiated by CIRT (**a**) and proton (**b**), and dose volume histogram (**c**)

double strand breaks at the carbon ion Bragg peak. The group at the Heidelberg Ion Beam Therapy Center (HIT) in Germany performed colony formation assays in four HCC cell lines (HepG2, HuH7, Hep3B, and PLC) and found RBEs in the range of 2.1–3.3 compared with photons. From cell survival data, α- and β-values were calculated by linear-quadratic model. As shown in Table 14.2, α-values of carbon ion

Table 14.2 α- and β-values from colony formation assay for four hepatocellular carcinoma cell lines

Beam	Parameter	Cell line			
		HepG2	Hep3B	HuH7	PLC
Photons	α	0.1482	0.3966	0.2973	0.3817
	β	0.0927	0.02301	0.03963	0.01244
Caron ion	α	1.733	0.8659	1.892	1.531
	β	−0.1685	0.4962	−0.1272	−0.07204

Adapted from Habermehl D [10]

increased, and β-values of carbon ion decreased for all four cell lines, indicating that the loading of lethal damage increased and the sublethal damage decreased. The change of α- and β-values implies that CIRT yields more DNA double-strand breaks than photon [10]. However, in the entrance dose area, the RBE is a little higher than 1. Moreover, cell kill from carbon ions at the depth of the "Bragg peak" does not rely on the presence of oxygen [11]. Thus, hypoxic tumor cells can be killed effectively and the oxygen enhance ratio (OER) decreased to 1.5–2. Overall, carbon ions have much stronger cell killing effects than photons and protons for X-ray-resistant tumor cells, including S and G_0 phase cells, hypoxic cells, and intrinsically resistant tumor cells. At the time of diagnosis, the majority of HCCs are large in size and likely contain a large proportion of hypoxic tumor cells. Therefore, use of CIRT may potentially further improve the local control of HCC, especially for large HCCs with a significant necrotic component.

14.3 The Technical Challenges in CIRT for HCC

14.3.1 Target Motion Control

There are several ways to control for motion of liver tumors including active breathing control (ABC) and abdominal compression. Additionally, respiratory gating devices have also been used to control for target motion in particle therapy. The Anzai respiratory gating system, a Japanese product, has been used in Japan and many other centers for protons and carbon ion therapy. The patient's breathing pattern is monitored by a pressure sensor mounted on a belt, which is fastened to the patient's abdomen. When radiation is being delivered, Anzai continues to monitor the patient's breathing phases and automatically sends signals to the synchrotron to trigger the ion beam on and off according to a predetermined gating window. The patient should be trained well to cooperate with Anzai and to keep a regular breathing rate. Before starting Anzai gated irradiation, we monitor the patient's respiratory pattern using an online X-ray fluoroscopic imaging system in our treatment room to make sure that the breathing amplitude and rate detected by Anzai correspond to the internal target motion. It is critical to ensure synchronization between breathing and internal target motion. In our practice, monthly quality

assurance for the Anzai device and good training of the patient can ensure optimal Anzai gating matching.

In order to decrease irradiation to the healthy liver, a narrow gating window should be chosen. From 4D-CT images, the gating window is selected, typically at the end of exhalation phase, e.g., from 40% of exhalation to 40% of inhalation, which provides a dose delivery time of 2–3 s. The ITV is formed by fusing CTVs at 40% exhalation, at end exhalation, and at 40% inhalation. When choosing the gating window, it is important to account for the interplay effect in the pencil beam scanning approach (detailed below). This experiment simulates the moving target in a phantom. A number of films were placed in a moving target to measure the target dose homogeneity. The target dose homogeneity becomes worse with increasing target motion range. However, the homogeneity was acceptable until the target motion reached 5.9 mm. Finally, we decided that the residual target motion in the gating window should be <5 mm for daily practice (Huang ZJ, et al. unpublished data).

14.3.2 The Interplay Effect: Rescanning

The technique of pencil beam scanning is the best way to deliver dose uniformly and conformally and sufficiently to protect OARs. However, it presents a great challenge for moving targets because of the so-called interplay effect, which introduces dose delivery uncertainty with poor dose homogeneity. To deal with the interplay effect, a beam rescanning technique was explored.

Mori in NIRS developed the rescanning approach for pencil beam scanning of carbon ion therapy, layered phase-controlled rescanning (PCR), and evaluated dose distribution simulated for various numbers of PCR for 30 liver cancers. It was found that PCR provided satisfactory dose homogeneity to the target. The homogeneity index (HI) decreased from 4.6 ± 1.2 (ungated) and 2.9 ± 1.5 (gated) to 0.5 ± 0.9 (ungated) and 1.2 ± 0.6 (gated), respectively, after eight rounds of PCR. In other words, a rescanning approach improved dose homogeneity, which partly accounted for the interplay effect. When the rescanning approach was used in combination with respiratory gating, HI was further improved as shown above [12].

Because it is nearly impossible to align the patient's breathing pattern with the simulation 4D-CT, Mori further studied irregular breathing. They designed a gating plan based on the first breath phase but calculated the target dose delivered by eight PCR on the irregular breathing pattern from real respiratory patterns in ten HCC patients. The study showed that D95 (lowest dose encompassing 95% of CTV) from the irregular breath treatment was 97.6 ± 0.5% and D95 from the planning dose was 98.5 ± 0.4%. Dmax/Dmin within the CTV was 1.6 ± 0.6% from the irregular breath treatment and 0.7 ± 0.2% from the planning. The above deviations can be considered acceptable. Therefore, the rescanning technique could possibly resolve the negative interplay effect for the moving target, even under irregular breathing [13].

Sometimes, PCR could not be completed within a single gating window due to the particular irradiation specifications, such as a large layer size, in which case the iso-energy layer has to be completed using the next gating window. In these

situations, the effect of rescanning is effectively nullified. NIRS proposed that the dose rate was adjusted to irradiate the number of rescans within multiple gating windows repeatedly until the total prescribed dose was given within a single gating window [14].

To deal with the interplay effect, another method to increase the scanning spot was proposed by GSI and HIT in Germany. They performed 4D dose calculation for treatment plans with variable beam parameters, including lateral raster spacing, beam spot (full width at half maximum), iso-energy slice spacing, and gating window. The assessed dosimetric parameters were under- and overdose, dose homogeneity, and DVH. Their study concluded that an increased beam spot size/lateral raster spacing could significantly mitigate the dose heterogeneities induced by the interplay effect [15].

14.4 Clinical Results for Application of CIRT for HCC

NIRS is the first hospital to treat HCC with CIRT in the world. Since 1995, they have carried out a series of prospective clinical trials to find the optimal dose and fractionation of CIRT for HCC. In 2004, they reported the results of 24 HCC treated by CIRT as part of a dose escalation study. The doses were given in 15 fractions over 5 weeks. During a median follow-up of 71 months, no severe adverse effects and no treatment-related deaths occurred. The local control (LC) and overall survival (OS) rates were 92% and 92%, 81% and 50%, and 81% and 25% at 1 year, 3 years and 5 years, respectively [16]. In 2010, they again reported on 64 HCCs irradiated with carbon ion to 52.8 GyE in four fractions. The 5-year OS and LC were 22.2% and 87.8% in HCC close to the porta hepatis and 34.8% and 95.7% in HCC distant from the hepatis, respectively. No patients developed biliary stricture [17]. In their book *Carbon Ion Radiotherapy* published in 2014, they reported on 133 HCC treated by CIRT with two fractions. 92% of patients were Child-Pugh A and 8% Child-Pugh B, and 87% were UICC stage 1–2 and 23% of stage IIIa and IVa. The median maximum tumor diameter was 42 mm (14–140 mm). The carbon ion dose ranged from 32 GyE to 45 GyE in two fractions. Acute toxicity was slight with only four cases of grade 3 hepatic toxicity and no other grade 3 and grade 4–5 toxicity, including late toxicity. For the higher-dose group (45.0 GyE) and the lower-dose group (≦42.8 GyE), the LC rates were 98% and 90% at 1 year and 83% and 76% at 3 years, respectively. The OS rates were 95% and 96% at 1 year and 71% and 59% at 3 years in the higher-dose group (45.0 GyE) and the lower-dose group (≦42.8 GyE), respectively [18, 19].

HIBMC reported on the treatment of HCC patients with protons or carbon ion beams. There were 242 HCC patients irradiated with protons to 52.8–84.0 GyE in 4–38 fractions and 101 HCC patients treated with carbon ions to 52.8–76.0 GyE in 4–20 fractions. The 5-year LC and OS rates for all patients were 90.8% and 38.2%, respectively. The 5-year LC rates were 90.2% and 93%, and the 5-year OS were 38% and 36.3%, respectively, for proton and carbon ion. No patients died of treatment-related toxicities [20].

Heidelberg Ion Therapy Center (HIT) in Germany published their protocol of a dose escalation study of carbon RT for HCC in 2011. They planned to give a treatment scheme of 40–56 GyE with fraction size of 10–14 GyE [21]. In 2013, they reported the preliminary results of six patients from the first dose level (40 GyE in 10 fractions). No severe adverse events occurred, and the LC rate was 100% with a median follow-up time of 11 months [22].

14.5 Practice in Shanghai Proton and Heavy Ion Center for HCC

In our center, the treatment strategies for technically unresectable and medically inoperable HCC include the use of combined transcatheter arterial chemoembolization (TACE) and particle irradiation, including proton, CIRT, or combination of proton and CIRT. Particle irradiation should be started after 2–4 cycles of TACE. The advantage of TACE prior to irradiation includes the following: (1) subclinical intrahepatic spreading could be detected by arteriography and injected iodine, (2) arteriography and the deposited iodine aid in contouring GTV margin, and (3) the deposited iodine also serves as a marker for image-guided radiation. The interval between TACE and particle irradiation should be at least 1 month based on our experience. More cycles of TACE can be considered after particle therapy, if patients can tolerate it. Anti-hepatitis virus agent is strongly recommended before, during, and after particle therapy for HCC associated with hepatitis.

Management of target motion with ABC involves a breath hold after deep inspiration. However, the deviation of reproducibility of the target position under ABC should be added to form an ITV. If the patient cannot cooperate with ABC, the patient can be trained for Anzai gating. The residual motion in the gating window is limited to less than 5 mm. When both above methods fail, abdominal compression can be used, but still the residual tumor motion should be less than 5 mm after abdominal compression.

For accurate delineation of GTV, the necessary images include arteriography CT with oral GI contrast, MRI with contrast, and PET/CT. To measure target motion, a 4D-CT is needed for patients with Anzai gating and abdominal compression, and the target reproducibility should be evaluated by fluoroscopy in a conventional simulator.

14.5.1 Target Volume

The definitions for the target are:

(1) GTV includes the gross tumor shown on images.
(2) CTV includes an extra margin of 5 mm added to GTV.
(3) ITV includes CTV plus appropriate margin depending on the deviation of target reproducibility for ABC, the fused CTVs from Anzai gating windows, or the fused CTVs from the end of inhalation and the end of exhalation for abdominal compression.

(4) PTV includes 3–5 mm added to ITV with additional margin in the beam axis directions.

The deposited iodine inside tumor should be overridden with soft tissue density before dose calculation.

The deposited iodine inside the tumor can be used for image guidance. When no iodine is deposited, insertion of fiducials is necessary adjacent to the tumor. After the patient is set up, two orthogonal films by kilovoltage X-ray are taken for position verification.

14.5.2 Verification

Several verification steps are undertaken before treatment. First, it is mandatory to have the plan verified by a group of 24 ion chambers in a water phantom prior to implementing CIRT. Moreover, immediately after irradiation, the patient is moved to PET/CT for PET scanning, and it is scanned on a flatbed table, in the same position as treatment with immobilization device. Figure 14.5 shows a PET image taken about 10 min after completion of 10 GyE of CIRT in an HCC patient. The verification performed in vivo only involved a geometric dose distribution, not a real biological dose distribution.

For CIRT fractionation, although Japanese data showed the optimal dose for controlling HCC, we are not able to implement this directly from their experience because of the different biological models used to convert the physical dose to biological dose. In Japan, the microdosimetric kinetic model (MKM) is used,

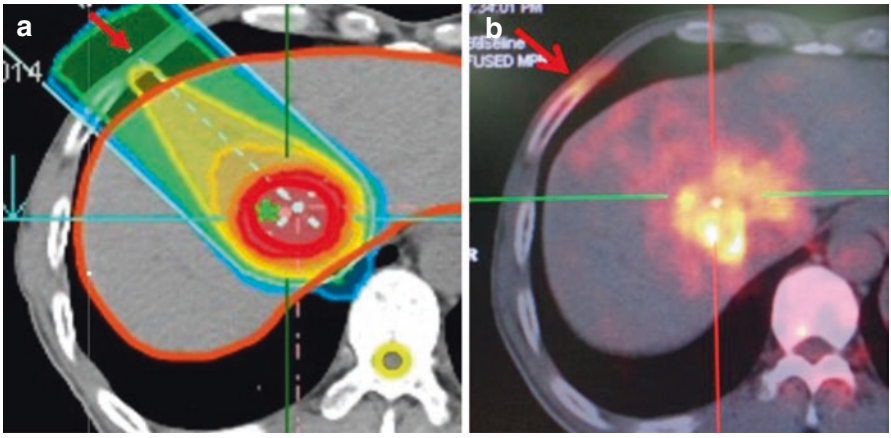

Fig. 14.5 PET image after 10 GyE of carbon ion irradiation for a hepatocellular carcinoma. (**a**) Biological dose distribution: *thick red line*, GTV; *thin red line*, 10 GyE. (**b**) PET image taken 10 min after 10 GyE of carbon ion

whereas, the local effect model (LEM) is used in HIT and our center. The same physical doses are converted to different biological doses by MKM and LEM [23, 24]. Therefore, the biological dose equivalent to ^{60}Cobalt (GyE) is really not equal using the two methods. We have carried out a dose escalation study again to find the appropriate dose/fractionation in SPHIC. Our aim is to deliver dose of BED_{10} of 100.

The following data are still under investigation in SPHIC. They are experimental and need to be confirmed. We would like to warn the readers to be very cautious in citing them for their practice.

The investigated fractionations for HCC were 5.5–6.5 GyE per fraction for ten fractions in 2 weeks for HCC ≥ 5 mm away from the GI tract and for tumors within 5 mm from the GI tract the combined proton of 50 GyE in 25 fractions and carbon ion of 15 GyE in five fractions until proton of 18 GyE in nine fractions and carbon ion of 45 GyE in 15 fractions.

For OAR dose constrains in CIRT for HCC, there has not been any clear data published yet in the literature. Our OAR dose constraints for 5.5–6.5 GyE/fraction are listed in Table 14.3, which are based on photon stereotactic body radiation (SBRT). Table 14.4 is for conventional fraction (2–3 GyE/fraction).

Table 14.3 OAR dose constrains for tumor located ≥ 5 mm away from the GI tract with 5.5–6.5 GyE per fraction

Liver	Normal liver volume of >700 mL, mean dose to normal liver[a] <15 GyE, V21 < 33%, V15 < 50% When normal liver volume of <700 mL, V17 < 70%
Kidney	Mean dose <12 GyE, V15 < 33%
Spinal cord	Maximum <27 GyE
Stomach	Maximum <32 GyE, V21 < 5 cm^3
Duodenum	Maximum <33 GyE
Small bowel	Maximum <34 GyE
Colon	Maximum <36 GyE

[a]Whole liver volume—GTV

Table 14.4 OAR dose constrains for tumors located <5 mm away from the GI tract with 2–3 GyE/fraction

Liver	Liver without cirrhosis, mean dose to normal liver[a] <30 GyE; liver with cirrhosis (Child-Pugh A), mean dose to normal liver <23 GyE
Stomach	V58 GyE < 0.03 mL; V50GyE < 5 mL; V45 GyE < 30 mL
Duodenum	V59 GyE < 0.03 mL; V56GyE < 5 mL; V45 GyE < 30 mL
Small bowel	V58 GyE < 0.03 mL; V50GyE < 10 mL; V45 GyE < 30 mL
Kidney	Single kidney, V18 < 80%; both kidneys, one >20 GyE and the other V18 < 10%
Spinal cord	Maximal <45 GyE, PRV V50 GyE < 1%

[a]Whole liver volume—GTV

Conclusion

(1) The clinical outcomes obtained with CIRT for HCC recently are encouraging.
(2) The technique of pencil beam scanning to treat HCC in CIRT needs further development.
(3) The optimal dose fractionation of CIRT for HCC and dose constraints for OARs should be further investigated based on biological models.
(4) CIRT to treat HCC is not yet in a fully mature stage and requires more evidence from clinical data.

References

1. Liang SX, Zhu XD, Xu ZY, et al. Radiation-induced liver disease in three-dimensional conformal radiation therapy for primary liver carcinoma: the risk factors and hepatic radiation tolerance. Int J Radiat Oncol Biol Phys. 2006;65(2):426–34.
2. Xu ZY, Liang SX, Zhu J, et al. Prediction of radiation-induced liver disease by Lyman normal-tissue complication probability model in three-dimensional conformal radiation therapy for primary liver carcinoma. Int J Radiat Oncol Biol Phys. 2006;65(1):189–95.
3. Zhao JD, Jiang GL, Hu WG, et al. Hepatocyte regeneration after partial liver irradiation in rats. Exp Toxicol Pathol. 2009;61(5):511–8.
4. Ren ZG, Zhao JD, Gu K, et al. Hepatic proliferation after partial liver irradiation in rat. Mol Biol Rep. 2012;39(4):3829–36.
5. Gu K, Lai ST, Ma NY, et al. Hepatic regeneration after sublethal partial liver irradiation in cirrhotic rats. J Radiat Res (Tokyo). 2011;52(5):582–91.
6. Gu K, Zhao JD, Ren ZG, et al. A natural process of cirrhosis resolution and deceleration of liver regeneration after thioacetamide withdrawal in a rat model. Mol Biol Rep. 2011;38(3):1687–96.
7. Fokas E, Kraft G, An H, Engenhart-Cabillic R. Ion beam radiobiology and cancer: time to update ourselves. Biochim Biophys Acta. 1796;2009:216–29.
8. Allen C, Borak TB, Tsujii H, et al. Heavy charged particle radiobiology: using enhanced biological effectiveness and improved beam focusing to advance cancer therapy. Mutat Res. 2011;711:150–7.
9. Furusawa Y. The characteristics of carbon ion radiotherapy. In: Tsujii H, Kamada T, Shirai T, Noda K, Tsuji H, Karawawa K, editors. Carbon ion radiotherapy. Japan: Springer; 2014. p. 25–37.
10. Habermehl D, Ilicic K, Dehne S, et al. The relative biological effectiveness for carbon and oxygen ion beams using the raster-scanning technique in hepatocellular carcinoma cell lines. PLoS One. 2014;9(12):e113591.
11. Bassler N, Toftegaard J, Luhr A, et al. LET-painting increases tumor control probability in hypoxic tumors. Acta Oncol. 2014;53:25–32.
12. Mori S, Zenklusen S, Inaniwa T, et al. Conformity and robustness of gated rescanned carbon ion pencil beam scanning of liver tumors at NIRS. Radiother Oncol. 2014;111:431–6.
13. Mori S, Inaniwa T, Furukawa T, et al. Amplitude-based gated phase-controlled rescanning in carbon-ion scanning beam treatment planning under irregular breathing conditions using lung and liver 4DCTs. J Radiat Res. 2014;55:948–58.
14. Ogata S, Mori S, Yasuda S. Extended phase-correlated rescanning irradiation to improve dose homogeneity in carbon-ion beam liver treatment. Phys Med Biol. 2014;59:5091–9.
15. Richter D, Graeff C, Jakel O, et al. Residual motion mitigation in scanned carbon ion beam therapy of liver tumors using enlarged pencil beam overlap. Radiother Oncol. 2014;113:290–5.

16. Kato H, Tsujii H, Miyamoto T, et al. Results of the first prospective study of carbon ion radiotherapy for hepatocellular carcinoma with liver cirrhosis. Int J Radiat Oncol Biol Phys. 2004;59(5):1468–76.
17. Imada H, Kato H, Yasuda S, et al. Conparison of efficacy and toxicity of short-course carbon ion radiotherapy for hepatocellular carcinoma depending on their proximity to the porta hepatis. Radiother Oncol. 2010;96:231–5.
18. Tsujii H, Kamada T, Shirai T, et al. Carbon-ion radiotherapy: principles, practices, and treatment planning. Japan: Springer; 2014. p. 213–8.
19. Imada H, Kato H, Yasuda S, et al. Compensatory enlargement of the liver after treatment of hepatocellular carcinoma with carbon ion radiotherapy - relation to prognosis and liver function. Radiother Oncol. 2010;96:236–42.
20. Komatsu S, Fukumoto T, Demizu Y, et al. Clinical results and risk factors of proton and carbon ion therapy for hepatocellular carcinoma. Cancer. 2011;117(21):4890–904.
21. Combs SE, Habermehl D, Ganten T, et al. Phase I study evaluating the treatment of patients with hepatocellular carcinoma (HCC) with carbon ion radiotherapy: the PROMETHEUS-01 trail. BMC Cancer. 2011;11:67.
22. Habermehl D, Debus J, Ganten T, et al. Hypofractionated carbon ion therapy delivered with scanned ion beam for patients with hepatocellular carcinoma - feasibility and clinical response. Radiat Oncol. 2013;8:59.
23. Steinstrater O, Grun R, Scholz U, et al. Mapping of RBE-weighted doses between HIMAC and LEM based treatment planning system for carbon ion therapy. Int J Radiat Oncol Biol Phys. 2012;84(3):854–60.
24. Fossati P, Molinelli S, Matsufuji N, et al. Dose prescription in carbon ion radiotherapy: a planning study for compare NIRS and LEM approaches with a clinically-oriented strategy. Phys Med Biol. 2012;57:7543–54.